INTERNATIONAL JOURNAL OF
NUMERICAL ANALYSIS AND MODELING
Volume 16, Number 2, Pages 210–224

A NEW *A POSTERIORI* ERROR ESTIMATE FOR THE INTERIOR PENALTY DISCONTINUOUS GALERKIN METHOD

WEI YANG, LULING CAO, YUNQING HUANG, AND JINTAO CUI*

Abstract. In this paper, we develop the adaptive interior penalty discontinuous Galerkin method based on a new *a posteriori* error estimate for the second-order elliptic boundary-value problems. The new *a posteriori* error estimate is motivated from the smoothing iteration of the m-time Gauss-Seidel iterative method, and it is used to construct the adaptive finite element method. The efficiency and robustness of the proposed adaptive method is demonstrated by extensive numerical experiments.

Key words. Interior penalty discontinuous Galerkin method, *a posteriori* error estimate, adaptive finite element methods, Gauss-Seidel iterative method.

1. Introduction.

The finite element method (**FEM**) is one of the most important computational tools in the field of science and engineering. The discontinuous Galerkin (**DG**) method is an innovation, improvement and development of the **FEM**. Since the **DG** method has advantages in parallel computing of the adaptive finite element method (**AFEM**), it has been favored by researchers and gradually become one of the important numerical methods in solving all kinds of partial differential equations. The **DG** method and theory have achieved fruitful results in recent years. The interior penalty discontinuous Galerkin (**IPDG**) method belongs to the family of symmetric **DG** methods. It has locally conservation, stability and high-order accuracy which can easily handle complex geometries, irregular meshes with hanging nodes and approximations with polynomials of different degrees in different elements. In 1982, Arnold [2] introduced the first **IPDG** method for heat equations, and now this method has already been applied in engineering increasingly, especially in the computational electromagnetics. For example, it's used in solving Maxwell's equations in cold plasma and dispersive media [17, 18], indefinite time-harmonic Maxwell's equations [16], compressible Navier-Stokes equations [15] and Helmholtz equations with spatially varying wavenumber [11], etc. The construction of a reliable and efficient error estimator is essential to the success of adaptive algorithms. In general, engineering calculations are mainly based on the first or second order finite element methods, and engineers hope to have a better precision for these low-order finite elements. However, most of the time the exact solutions are unknown, and the errors can not be calculated directly. In such cases, many researchers pay their attention to *a posteriori* error estimates, and the real errors can be better approximated by post-processing techniques with the obtained finite element solutions. The *a posteriori* error estimate and the **AFEM** were first introduced by [4]. Since the late 1980s, the residual type *a posteriori* error estimate [8], the recovery type *a posteriori* error estimate [26], the *a posteriori* error estimate based on the hierarchic basis [6, 7], a new *a posteriori* error estimate for **AFEM**

Received by the editors September 30, 2017 and, accepted February 5, 2018.
2000 *Mathematics Subject Classification.* 65N15, 65N30, 35J20.
*Corresponding author.

[19] and a series of works on the *a posteriori* error estimation [1, 5, 24, 25] have been put forward one after another.

With the rapid development of the **DG** theory, the *a posteriori* error estimation theory based on **DG** methods arises. There are a large number of numerical and theoretical literatures on **AFEM**, and many scholars also put forward to different kinds of *a posteriori* error estimates for various problems. Since 2000, much research work on the *a posteriori* error estimation has been developed including the residual *a posteriori* error estimate for the **DG** approximation of second-order elliptic problems [20], and the *a posteriori* error estimations and mesh adaptivity strategies for **DG** methods applied to diffusion problems [22]. The **IPDG** method has many good properties, which render it ideal to be used with the local mesh refinement and the independent selection of the polynomial degree in each element. Those distinct advantages make the computation of finite elements more efficient and flexible. At the same time, owing to the degrees of freedom for each unit are less than other **DG** methods, the **IPDG** formulation is relatively easier to be paralleled. In this paper we aim to propose a new *a posteriori* error estimate for the **IPDG** method by handling the numerical solution in a simple way. It is shown to be a simple and efficient way to improve the approximation accuracy of the numerical solution with less computational cost.

In this paper, we consider the **IPDG** method for a second-order elliptic boundary-value problem. We present a new *a posteriori* error estimator with m-time Gauss-Seidel iterations in an energy norm (cf. G-norm below) and use it to construct the **AFEM**. In particular, on the current triangulation $\mathcal{T}_h$, we solve the equation to obtain the **DG** solution u_h, then globally refine $\mathcal{T}_h$ to obtain an auxiliary mesh $\mathcal{T}_{h/2}$. On the fine mesh, we use a simple smoother such as the Gauss-Seidel iterations with u_h as the initial value. After m-time iterations, we obtain an approximation $u_{h/2,m}$ of the **DG** solution $u_{h/2}$ on the fine mesh $\mathcal{T}_{h/2}$. We then take $\|u_{h/2,m} - u_h\|_G$ as the *a posteriori* error estimator to guide the mesh refinement on $\mathcal{T}_h$. In practice, it only needs a small number of smoothing steps to obtain an efficient *a posteriori* error estimator, hence the computational cost is relatively small.

The rest of the paper is organized as follows. In section 2, we propose a new *a posteriori* error estimator and then describe the **AFEM** algorithm with it for second-order elliptic boundary-value problem. We present some numerical results to show the efficiency of the new *a posteriori* error estimator and the performance of the corresponding **AFEM** algorithm in section 3.

2. The New *A Posteriori* Error Estimate.

2.1. The Interior Penalty Discontinuous Galerkin Method. In this work, we consider the following second-order elliptic boundary-value problem:

$$-\nabla \cdot (a\nabla u) + bu = f \quad \text{in } \Omega, \tag{1}$$

$$u = g \quad \text{on } \partial\Omega, \tag{2}$$

where Ω is a bounded domain of $\mathbb{R}^2$, $\partial\Omega$ is the Lipschitz boundary. For the sake of simplicity and easy presentation, we consider the homogeneous boundary condition, i.e., $g = 0$ and Ω is assumed to be a convex polygonal domain. The coefficient matrix $a = (a_{ij})$ is symmetric and uniformly positive definite, $a_{ij} \in L^\infty(\Omega)$, $b \in L^\infty(\Omega)$ and f is a given function in $L^2(\Omega)$.

We rewrite the model problem (1) and (2) into first order mixed equations as follows:

$$\boldsymbol{\sigma} = a\nabla u, \quad -\nabla\cdot\boldsymbol{\sigma} + bu = f, \quad in\ \Omega; \quad u = 0, \quad on\ \partial\Omega.$$

For any triangle $K \subset \Omega$, the first order mixed variational form reads: Find $u \in H^1(K)$, $\boldsymbol{\sigma} \in H(\mathrm{div}; K)$ such that

$$\int_K a^{-1}\boldsymbol{\sigma}\cdot\boldsymbol{\tau} d\boldsymbol{x} = -\int_K u\nabla\cdot\boldsymbol{\tau} d\boldsymbol{x} + \int_{\partial K} u\boldsymbol{\tau}\cdot\boldsymbol{n} ds \qquad \forall\ \boldsymbol{\tau}\in H(\mathrm{div}; K), \tag{3}$$

$$\int_K \boldsymbol{\sigma}\cdot\nabla v d\boldsymbol{x} + \int_K buv d\boldsymbol{x} = \int_K fv d\boldsymbol{x} + \int_{\partial K} v\boldsymbol{\sigma}\cdot\boldsymbol{n} ds \qquad \forall\ v\in H^1(K), \tag{4}$$

where $H(\mathrm{div}; K) := \{\boldsymbol{v} \in [L^2(K)]^2, \mathrm{div}\boldsymbol{v} \in L^2(K)\}$ and $\boldsymbol{n}$ is the outward normal unit vector of ∂K. Let $\mathcal{T}_h = \cup\{K\}$ be a shape-regular triangulation of region Ω, $h = max\{h_K : K \in \mathcal{T}_h\}$ is the partition diameter, h_K is the diameter of cell K, $\Gamma_h = \cup\{e \subset \partial K : K \in \mathcal{T}_h\}$ denotes the collection of all triangles edges and $\Gamma_h^0 = \Gamma_h \setminus \partial\Omega$ is interior edges of these triangles. The discontinuous linear finite element space S_h is defined by

$$S_h := \{v \in L^2(\Omega) : v|_K \in P_1(K), \forall\ K \in \mathcal{T}_h\},$$

and the discontinuous finite element vector space is $V_h := [S_h]^2 = \{\boldsymbol{\tau} \in [L^2(\Omega)]^2 : \boldsymbol{\tau}|_K \in [P_1(K)]^2, \forall\ K \in \mathcal{T}_h\}$.

According to the mixed variational form, the elliptic boundary-value problem is approximately solved by finding $(u_h, \boldsymbol{\sigma_h}) \in S_h \times V_h$, such that

$$\int_K a^{-1}\boldsymbol{\sigma}_h\cdot\boldsymbol{\tau}_h d\boldsymbol{x} = -\int_K u_h\nabla\cdot\boldsymbol{\tau}_h d\boldsymbol{x} + \int_{\partial K} \hat{u}_h\boldsymbol{\tau}_h\cdot\boldsymbol{n} ds \qquad \forall\ \boldsymbol{\tau}_h\in V_h, \tag{5}$$

$$\int_K \boldsymbol{\sigma}_h\cdot\nabla v_h d\boldsymbol{x} + \int_K bu_hv_h d\boldsymbol{x} = \int_K fv_h d\boldsymbol{x} + \int_{\partial K} v_h\hat{\boldsymbol{\sigma}}_h\cdot\boldsymbol{n} ds \qquad \forall\ v_h\in S_h, \tag{6}$$

where $\hat{u}_h = \hat{u}_h(u_h, \boldsymbol{\sigma}_h)$, $\hat{\boldsymbol{\sigma}}_h = \hat{\boldsymbol{\sigma}}_h(u_h, \boldsymbol{\sigma}_h)$ are numerical fluxes. They are approximations of u and $\boldsymbol{\sigma} = a\nabla u$ at element boundaries. It's necessary to introduce the jump $[[\cdot]]$ and the average $\{\cdot\}$ to handle the discontinuity of finite element functions crossing unit interfaces. Let $v \in H^1(\mathcal{T}_h) := \{v \in L^2(\Omega) : v|_K \in H^1(K), \forall\ K \in \mathcal{T}_h\}$, $e = \partial K_1 \cap \partial K_2$ denote the interface of adjacent triangles K_1, K_2 and $v_i = v|_{\partial K_i}$ denote the trace of v on the boundary of element K_i. $\boldsymbol{n}_i = \boldsymbol{n}|_{\partial K_i}$ is the outward normal unit vector on ∂K_i. For $v \in H^1(\mathcal{T}_h)$, the jump $[[v]]$ and the average $\{v\}$ are defined as follows:

$$[[v]] = v_1\boldsymbol{n_1} + v_2\boldsymbol{n_2}, \qquad \{v\} = \frac{1}{2}(v_1 + v_2), \quad e \in \Gamma_h^0.$$

For vector function $\boldsymbol{\tau} \in [H^1(\mathcal{T}_h)]^2$,

$$[[\boldsymbol{\tau}]] = \boldsymbol{\tau_1}\cdot\boldsymbol{n_1} + \boldsymbol{\tau_2}\cdot\boldsymbol{n_2}, \qquad \{\boldsymbol{\tau}\} = \frac{1}{2}(\boldsymbol{\tau_1} + \boldsymbol{\tau_2}), \quad e \in \Gamma_h^0.$$

If $e \subset \partial\Omega$, then let $[[v]] = v\boldsymbol{n}, \{v\} = v, [[\boldsymbol{\tau}]] = \boldsymbol{\tau}\cdot\boldsymbol{n}, \{\boldsymbol{\tau}\} = \boldsymbol{\tau}$.

We take $\hat{u}_h = \{u_h\}$ on Γ_h^0, $\hat{u}_h|_{\partial\Omega} = 0, \hat{\boldsymbol{\sigma}}_h = \{a\nabla_h u_h\} - \mu[[u_h]]$ on Γ_h, where $\mu = \lambda h_e^{-1}$ (the penalty parameter λ is taken to be sufficiently large), $h_e = diam(e)$, $e \in \Gamma_h$. The **IPDG** formulation [3] is defined as follows:

$$B_h(u_h, v_h) = \int_\Omega fv_h dx, \qquad \forall\ v_h \in S_h, \tag{7}$$

where

$$B_h(u_h, v_h) := \int_\Omega a\nabla_h u_h \cdot \nabla_h v_h d\boldsymbol{x} + \int_\Omega b u_h v_h d\boldsymbol{x} \\ - \int_{\Gamma_h} ([[u_h]] \cdot \{a\nabla_h v_h\} + \{a\nabla_h u_h\} \cdot [[v_h]])ds + \int_{\Gamma_h} \mu[[u_h]] \cdot [[v_h]]ds,$$

$\nabla_h = \nabla$ is the discrete gradient operator.

Let A^h denote the coefficient matrix of discrete equations for the **IPDG** scheme (7), i.e., then

$$B_h(u_h, v_h) = (A^h\boldsymbol{u}, \boldsymbol{v}), \qquad \forall\ u_h, v_h \in S_h, \tag{8}$$

where $\boldsymbol{u}, \boldsymbol{v} \in \mathbb{R}^N$ are vectors corresponding to u_h, v_h. We assume that $\{\psi_i : i = 1, 2, \dots N\}$ is the standard linear Lagrange basis in S_h, matrix A^h and vector F^h are defined as follows:

$$A^h_{ij} := B_h(\psi_j, \psi_i), \qquad F^h_i := f(\psi_i), \qquad i, j = 1, 2, \dots N,$$

The **IPDG** equations for (1) and (2) can be written as $A^hU = F^h$. Obviously, A^h is symmetrical positive definite matrix since $u_h = \sum_{i=1}^N u_i\psi_i$ and $U = (u_i)$.

We define the G-norm in Ω as follows:

$$\|v\|_G := (\sum_{K\in\mathcal{T}_h} \|a^{\frac{1}{2}}\nabla v\|^2_{L^2(K)} + \sum_{K\in\mathcal{T}_h} \|b^{\frac{1}{2}} v\|^2_{L^2(K)} \\ + \sum_{e\in\Gamma_h} \mu\|[[v]]\|^2_{L^2(e)} + \sum_{e\in\Gamma_h} \frac{1}{\mu}\|\{a\nabla v\}\|^2_{L^2(e)})^{\frac{1}{2}}.$$

Next we show the continuity and coerciveness of $B_h(u_h, v_h)$. We use the Cauchy-Schwarz inequality to give the estimates about the fourth term of $B_h(u_h, v_h)$, such that

$$\begin{aligned} |\sum_{e\in\Gamma_h} \int_e \{a\nabla u_h\} \cdot [[v_h]]ds| &= |\sum_{e\in\Gamma_h} \int_e \sqrt{\frac{1}{\mu}}\{a\nabla u_h\} \cdot \sqrt{\mu}[[v_h]]ds| \\ &\le (\sum_{e\in\Gamma_h} \frac{1}{\mu}\|\{a\nabla u_h\}\|^2_{L^2(e)})^{\frac{1}{2}} (\sum_{e\in\Gamma_h} \mu\|[[v_h]]\|^2_{L^2(e)})^{\frac{1}{2}} \\ &\le \|u_h\|_G \cdot \|v_h\|_G. \end{aligned} \tag{9}$$

Since,

$$\begin{aligned} B_h(v_h, v_h) &= \sum_{K\in\mathcal{T}_h} \int_K a\nabla v_h \cdot \nabla v_h d\boldsymbol{x} + \sum_{K\in\mathcal{T}_h} \int_K b v_h^2 d\boldsymbol{x} \\ &\quad - \sum_{e\in\Gamma_h} \int_e ([[v_h]] \cdot \{a\nabla v_h\} + \{a\nabla v_h\} \cdot [[v_h]])ds + \sum_{e\in\Gamma_h} \int_e \mu[[v_h]]^2 ds \\ &= \sum_{K\in\mathcal{T}_h} \|a^{\frac{1}{2}}\nabla v_h\|^2_{L^2(K)} + \sum_{K\in\mathcal{T}_h} \|b^{\frac{1}{2}} v_h\|^2_{L^2(K)} - 2\sum_{e\in\Gamma_h} \int_e [[v_h]] \cdot \{a\nabla u_h\}ds \\ &\quad + \sum_{e\in\Gamma_h} \mu\|[[v_h]]\|^2_{L^2(e)} \\ &= \|v_h\|^2_G - 2\sum_{e\in\Gamma_h} \int_e [[v_h]] \cdot \{a\nabla v_h\}ds - \sum_{e\in\Gamma_h} \frac{1}{\mu}\|\{a\nabla v_h\}\|^2_{L^2(e)}. \end{aligned}$$

Using the Cauchy-Schwarz inequality, we have

$$\begin{aligned}\sum_{e\in\Gamma_h}\int_e [[v_h]]\cdot\{a\nabla v_h\}ds &= \sum_{e\in\Gamma_h}\int_e \sqrt{\mu}[[v_h]]\cdot\sqrt{\frac{1}{\mu}}\{a\nabla v_h\}ds\\ &\le \frac{1}{2}(\sum_{e\in\Gamma_h}\frac{\mu}{2}\|[[v_h]]\|^2_{L^2(e)}+\sum_{e\in\Gamma_h}\frac{2}{\mu}\|\{a\nabla v_h\}\|^2_{L^2(e)})\\ &= \sum_{e\in\Gamma_h}\frac{\mu}{4}\|[[v_h]]\|^2_{L^2(e)}+\sum_{e\in\Gamma_h}\frac{1}{\mu}\|\{a\nabla v_h\}\|^2_{L^2(e)}.\end{aligned}$$

Therefore,

$$\begin{aligned}B_h(v_h,v_h)\ge&\|v_h\|^2_G-2(\sum_{e\in\Gamma_h}\frac{\mu}{4}\|[[v_h]]\|^2_{L^2(e)}+\sum_{e\in\Gamma_h}\frac{1}{\mu}\|\{a\nabla v_h\}\|^2_{L^2(e)})\\ &-\sum_{e\in\Gamma_h}\frac{1}{\mu}\|\{a\nabla v_h\}\|^2_{L^2(e)}\\ =&\|v_h\|^2_G-\frac{1}{2}\sum_{e\in\Gamma_h}\mu\|[[v_h]]\|^2_{L^2(e)}-3\sum_{e\in\Gamma_h}\frac{1}{\mu}\|\{a\nabla v_h\}\|^2_{L^2(e)}.\end{aligned}$$

Note that $h_K = O(h_e)$ and using the local trace inequality [12], we have

$$3\sum_{e\in\Gamma_h}\frac{1}{\mu}\|\{a\nabla v_h\}\|^2_{L^2(e)}\le\frac{C}{\mu}\sum_{K\in\mathcal{T}_h}h_K^{-1}\|a^{\frac{1}{2}}\nabla v_h\|^2_{L^2(K)}\le\frac{C}{\lambda}\sum_{K\in\mathcal{T}_h}\|a^{\frac{1}{2}}\nabla v_h\|^2_{L^2(K)}.$$

Therefore,

$$B_h(v_h,v_h)\ge\|v_h\|^2_G-max\{\frac{1}{2},\frac{C}{\lambda}\}\|v_h\|^2_G,$$

where the penalty parameter λ is taken to be sufficiently large, we have $\frac{C}{\lambda}<\frac{1}{2}$, then

$$B_h(v_h,v_h)\ge\frac{1}{2}\|v_h\|^2_G. \tag{10}$$

According to the Lax-Milgram theorem, the **IPDG** formulation (7) is well-posed.

2.2. The *A Posteriori* Error Estimator. Refine the triangle mesh $\mathcal{T}_h$ globally to get $\mathcal{T}_{h/2}$, then $S_h\subset S_{h/2}$. Let u_h and $u_{h/2}$ be the finite element solutions of $\mathcal{T}_h$ and $\mathcal{T}_{h/2}$. Since $\frac{\|u-u_h\|_G}{\|u-u_{h/2}\|_G}\to 2$, we have the formulas [10] as follows:

$$\frac{\|u-u_h\|_G}{\|u_{h/2}-u_h\|_G}\le\frac{\|u-u_{h/2}\|_G+\|u_{h/2}-u_h\|_G}{\|u_{h/2}-u_h\|_G}=\frac{\frac{1}{2}\|u-u_h\|_G}{\|u_{h/2}-u_h\|_G}+1,$$

$$\frac{\|u-u_h\|_G}{\|u_{h/2}-u_h\|_G}\le 2; \tag{11}$$

$$\frac{\|u-u_h\|_G}{\|u_{h/2}-u_h\|_G}\ge\frac{\|u-u_h\|_G}{\|u-u_{h/2}\|_G+\|u-u_h\|_G}=\frac{\|u-u_h\|_G}{\frac{1}{2}\|u-u_h\|_G+\|u-u_h\|_G},$$

$$\frac{\|u-u_h\|_G}{\|u_{h/2}-u_h\|_G}\ge\frac{2}{3}; \tag{12}$$

Therefore,

$$\frac{2}{3}\le\frac{\|u-u_h\|_G}{\|u_{h/2}-u_h\|_G}\le 2. \tag{13}$$

In conclusion, when $u_{h/2}$ is known, we could take $\|u_{h/2} - u_h\|_G$ as the *a posteriori* error estimator. Since the $u_{h/2}$ can be approximated by $u_{h/2,m}$ after m-time Gauss-Seidel iterations, we can replace the error estimator $\|u_{h/2} - u_h\|_G$ with $\|u_{h/2,m} - u_h\|_G$. By this means, the computation cost can be reduced greatly.

Given the finite element solution u_h on current triangulation $\mathcal{T}_h$, we can get the *a posteriori* error estimator by the following steps.

Step 1. Refine the current mesh $\mathcal{T}_h$ globally to get the fine mesh $\mathcal{T}_{h/2}$.

Step 2. Build the finite element space $S_{h/2}$ on the fine mesh $\mathcal{T}_{h/2}$, and get the corresponding stiffness matrix $A^{h/2}$ and load vector $F^{h/2}$.

Step 3. Taking the given finite element solution u_h as initial solution, solve the linear algebraic equations

$$A^{h/2}U = F^{h/2}.$$

by Gauss-Seidel iterative methods. After m-time iterations, we can get the approximation $U^m = (u_i^m)$ of $u_{h/2}$. Then we take

$$u_{h/2,m} = \sum_{i=1}^{N_{h/2}} u_i^m \psi_i,$$

where $N_{h/2}$ is the number of basis $\{\psi_i\}$ in $S_{h/2}$.

Step 4. For each $K \in \mathcal{T}_h$, calculate

$$\eta_{K,m} = \|u_h - u_{h/2,m}\|_{G,K}.$$

Finally we take $\eta_{h,m} = (\sum_{K\in\mathcal{T}_h} \eta_{K,m}^2)^{1/2}$ as the *a posteriori* error estimator.

2.3. Condition Numbers and the Smoothing Property. In this section we first consider the condition number of the **IPDG** scheme on adaptively refined meshes $\{\mathcal{T}_l : l \in \mathcal{N}\}$. A triangulation family $\{\mathcal{T}_l : l \in \mathcal{N}\}$ is said to be non-degenerate [21] if there exists a constant $\rho > 0$ such that for all $l \in \mathcal{N}$ and for all $K \in \mathcal{T}_l$, there is a ball of radius $\rho \cdot diam(K)$ contained in K. Assume the basis $\{\psi_i : i = 1, 2, \ldots N\}$ in S_h is a local basis, and

$$\max_{1\le i\le N} cardinality\{K \in \mathcal{T}_h, supp(\psi_i) \cap K \neq \varnothing\} \le C. \tag{14}$$

Then we can establish the following lemma, following the ideas in [19].

Lemma 2.1. *Suppose that the mesh $\mathcal{T}_h$ is non-degenerate. Let A^h denote the matrix corresponding to the inner product $B_h(\cdot,\cdot)$, i.e., $A_{ij}^h = B_h(\psi_i, \psi_j)$, where ψ_i $(i = 1, 2, \ldots N)$ are the standard linear Lagrange basis functions. Then the maximum eigenvalue λ_{max} of A^h is bounded by*

$$\lambda_{max} \le C. \tag{15}$$

Proof. Since $v = \sum_{i=1}^N v_i\psi_i$, we have

$$B_h(v, v) = V^T A^h V,$$

where $V = (v_i)$. Since $B_h(\cdot,\cdot)$ is bilinear, from the inverse estimate and (14), we have

$$B_h(v, v) \le C\|v\|_G^2 = C \sum_{K\in\mathcal{T}_h} \|v\|_{G,K}^2 \le C \sum_{K\in\mathcal{T}_h} \|v\|_{0,\infty,K}^2$$

$$\le C \sum_{K\in\mathcal{T}_h} \sum_{supp(\psi_i)\cap K\neq\varnothing} v_i^2 \le CV^T V.$$

Therefore, we can get (15). □

For solving the linear equations $AU = F$, a basic linear iterative method can be written as follows:

$$U^{k+1} = U^k + B(F - AU^k), \qquad k = 0, 1, 2 \dots, \tag{16}$$

with initial value is $U^0 \in R^n$. Take the (16) as the Richardson iterative scheme, i.e., $B = \frac{\omega}{\rho(A)} I$, where $\rho(A)$ is the spectral radius of matrix A, then

$$U^{k+1} = U^k + \frac{\omega}{\rho(A)}(F - AU^k), \qquad k = 0, 1, 2 \dots. \tag{17}$$

Take $\omega = 1$, $S = I - \frac{A}{\rho(A)}$, then (17) can be rewritten as

$$U^{k+1} = (I - \frac{A}{\rho(A)})U^k + \frac{1}{\rho(A)}F, \tag{18}$$

We then can establish the following theorem on the property of smoother S.

Theorem 2.1. *For the smoother S, we have*

$$\|S^m V\|_A \leq C m^{-1/2} \|V\|_0, \qquad \forall\ V \in R^n, \tag{19}$$

where $\|V\|_0 = (V, V)^{1/2}$ is the l^2 norm in R^n, and the A-norm is defined as follows:

$$\|V\|_A := (AV, V)^{1/2}.$$

Note that the A-norm corresponds to the linear system we wish to solve.

Proof. Since A is an symmetric positive definite matrix, we have $A\phi_i = \lambda_i \phi_i$ with $\lambda_{min} \leq \lambda_1 \leq \lambda_2 \leq \dots \leq \lambda_{max}, (\phi_i, \phi_j) = \delta_{ij}$. $\forall\ V \in R^n$, we can write it as

$$V = \sum_{i=1}^{n} v_i \phi_i,$$

Therefore,

$$S^m V = (I - \frac{1}{\rho(A)}A)^m V = \sum_{i=1}^{n} (1 - \frac{\lambda_i}{\lambda_{max}})^m v_i \phi_i,$$

and

$$\begin{aligned} \|S^m V\|_A^2 =& \lambda_{max} (\sum_{i=1}^{n} (1 - \frac{\lambda_i}{\lambda_{max}})^{2m} \frac{\lambda_i}{\lambda_{max}} v_i^2) \\ \leq& \lambda_{max} \{ \sup_{0 \leq x \leq 1} (1 - x)^{2m} x \} \sum_{i=1}^{n} v_i^2. \end{aligned} \tag{20}$$

Since

$$\sup_{0 \leq x \leq 1} (1 - x)^{2m} x \leq \frac{1}{2m + 1},$$

from (15) we have

$$\lambda_{max} \leq C.$$

Then, from the above inequalities, we obtain

$$\|S^m V\|_A^2 \leq C m^{-1} \|V\|_0^2.$$

□

In the following discussion, we investigate the smoothing property of Gauss-Seidel smoother on uniformly refined meshes. We solve the Poisson equation with the exact solution $u = r^{\frac{2}{3}} \sin(\frac{2}{3}\theta)$, $r = \sqrt{x^2 + y^2}$ on a L-shaped domain. We first obtain the **IPDG** solution u_h on $\mathcal{T}_h$, see the mesh in Figure 1(A), then we get $\mathcal{T}_{h/2}$ by globally refining $\mathcal{T}_h$. Set u_h as the initial value, and solve the problem (3.1) by executing m smoothing steps on the $\mathcal{T}_{h/2}$, see Figure 1(B). The result is plotted in Figure 1(C). It can be observed that the smoothing operator S admits the similar property on the locally refined meshes. It's obvious that we can get an approxima-

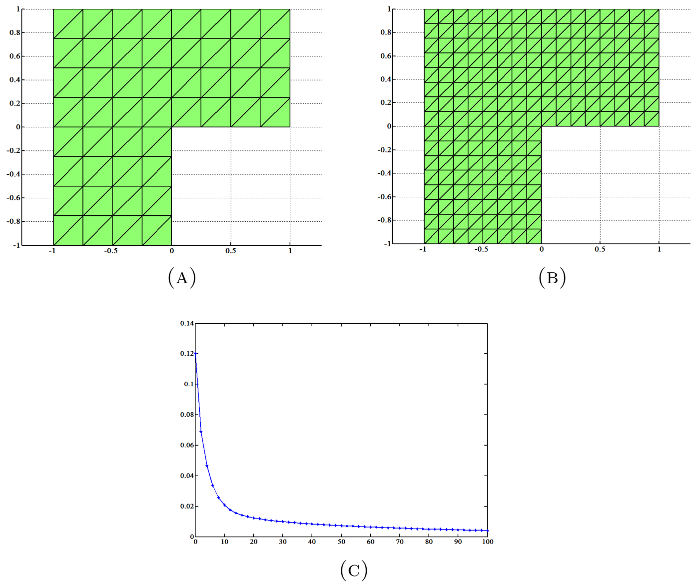

FIGURE 1. (A) initial mesh; (B) globally refined mesh; (C) Gauss-Seidel convergence history.

tion $u_{h/2,m}$ for $u_{h/2}$ at any accuracy with a larger m. And we know that the error between $u_{h/2}$ and $u_{h/2,m}$ is reduced quickly at the beginning of several iterative steps, then we need to do only a few smoothing steps to obtain an approximation $u_{h/2,m}$ for our *a posteriori* error estimator. It is observed from our numerical experiments in section 3 that $m = 5$ performs well enough.

3. Adaptive Algorithms and Numerical Examples.

Firstly, we introduce the **AFEM** with local mesh refinement which can be described as follow steps (see Figure 2):

$$\text{SOLVE} \quad \rightarrow \quad \text{ESTIMATE} \quad \rightarrow \quad \text{MARK} \quad \rightarrow \quad \text{REFINE}$$

Next we give some numerical examples to investigate and verify the effectiveness of the *a posteriori* error estimator based on the **IPDG** method in comparison with different iterative times, especially, we choose the times of iterations are $m = 5$, $m = 8$ and $m = 10$.

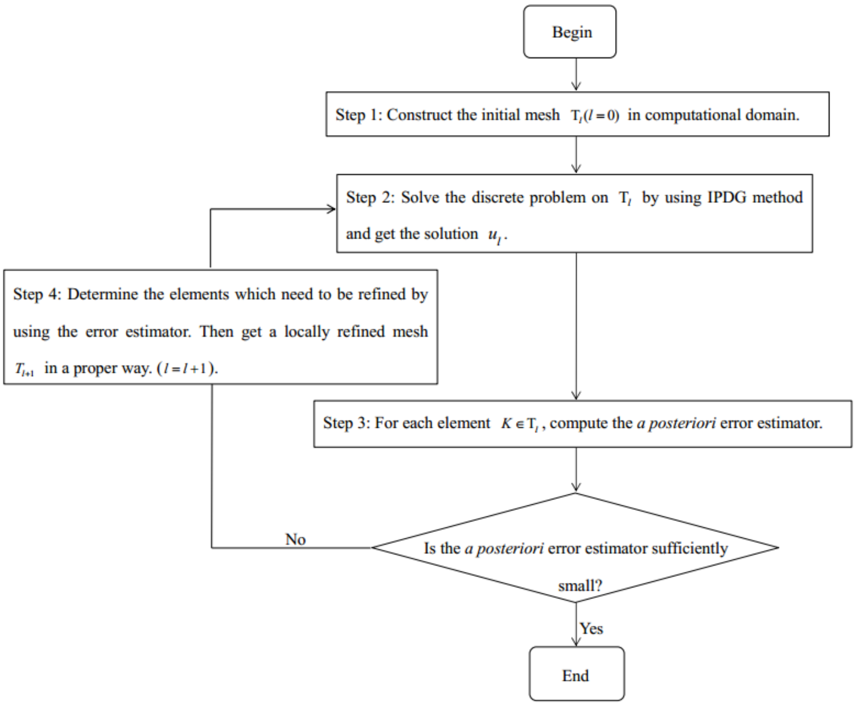

FIGURE 2. Adaptive algorithm.

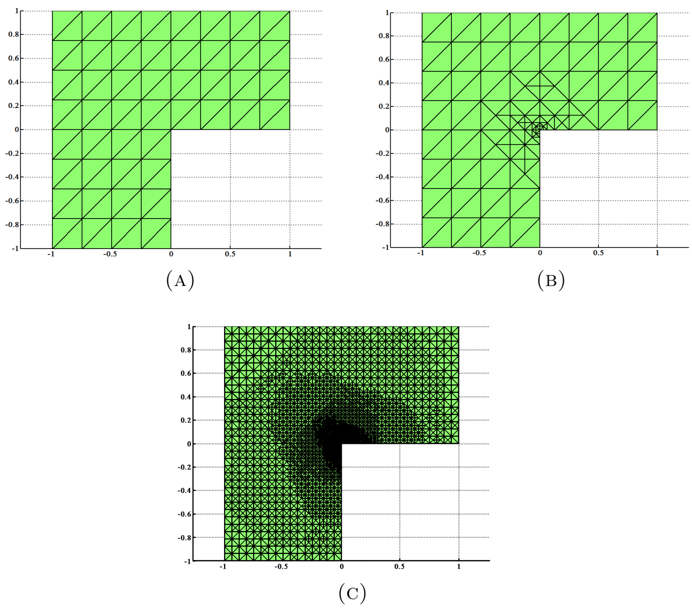

FIGURE 3. (A) initial mesh; (B) refined mesh after 10 refinements; (C) final mesh.

Investigate the model problem

$$
\begin{aligned}
-\Delta u &= f, \text{ in } \Omega, \\
u &= g, \text{ on } \partial\Omega,
\end{aligned}
$$

where $\Omega \subset \mathbb{R}^2$ is bounded domain with a Lipschitz boundary $\partial\Omega$. For each $K \in \mathcal{T}_h$, let

$$\eta_K = \|u_{h/2} - u_h\|_{G,K}, \qquad \eta_h = \|u_{h/2} - u_h\|_G.$$

Define the *a posteriori* error estimator in K as follows:

$$\eta_{K,m} = \|u_{h/2,m} - u_h\|_{G,K}, \qquad \eta_{h,m} = \|u_{h/2,m} - u_h\|_G.$$

In order to verify the accuracy of $\eta_{\cdot,m}$, we will use the indices θ_K, θ_h which are defined as follows:

$$\theta_K = \frac{\eta_{K,m}}{\|u - u_h\|_{G,K}}, \qquad \theta_h = \frac{\eta_{h,m}}{\|u - u_h\|_G}.$$

In all the numerical experiments, we use the bisection methods [23] to refine the local mesh and use Gauss-Seidel iteration as smoother. Considering $\eta_{h,m}$ as the error estimator, we use Matlab package iFEM [9] to perform the numerical tests.

Example 1. In this example, we solve the model problem (3.1) in L-shaped domain $\Omega = \{-1 \le x, y \le 1\} \setminus \{0 \le x \le 1, -1 \le y \le 0\}$, where $f = 0$. In this case, the exact solution is $u = r^{\frac{2}{3}} \sin(\frac{2}{3}\theta)$ where $r = \sqrt{x^2 + y^2}$. In this problem, we consider the 5, 8, 10 iterative steps respectively (see Figure 4). It can be observed that the effect of 5 iterative steps is better. The initial mesh, 10-time-refined mesh and final mesh are depicted in Figure 3. The index θ_h and errors of 5, 8, 10 iterations are shown in Figure 5. We can see $\|u - u_h\|_G = O(N^{-1/2})$, and the index θ_h is stable at some values.

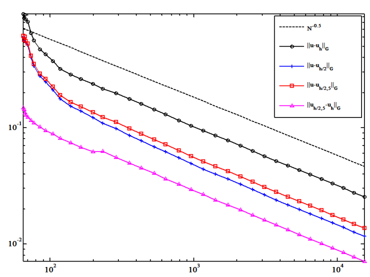

(A)

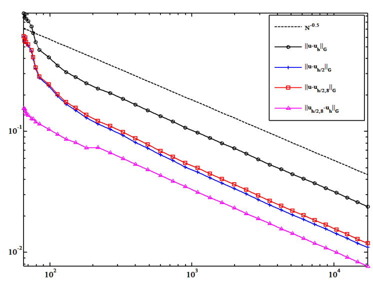

(B)

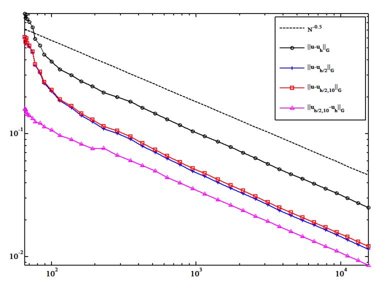

(C)

FIGURE 4. The convergence history of AFEM. (A) $m = 5$; (B) $m = 8$; (C) $m = 10$.

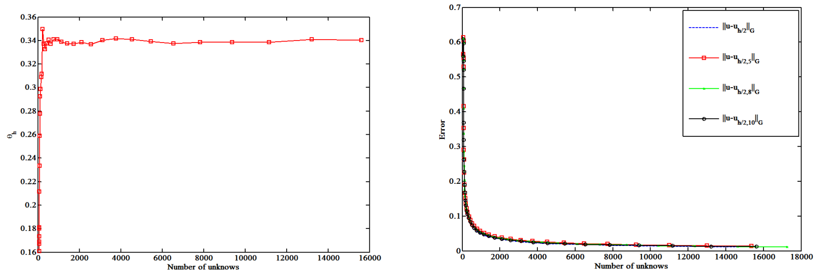

(A) (B)

FIGURE 5. (A) The index θ_h for $m = 5$. (B) Errors $||u - u_{h/2,m}||_G$ for $m = 5, 8, 10$.

Example 2. In this example, we solve the model problem (3.1) in $\Omega = [0,1] \times [0,1]$. The exact solution is

$$u = \frac{1}{1 + e^{-100(\sqrt{x^2+y^2}-0.75)}}.$$

The numerical tests are carried out by 5, 8, 10 iterations respectively (see Figure 7). From the figures, we observe that 5 iteration steps perform better. The initial mesh, 10-time-refined mesh and the final mesh are depicted in Figure 6. The index θ_h and errors of 5, 8, 10 iterations are shown in Figure 8.

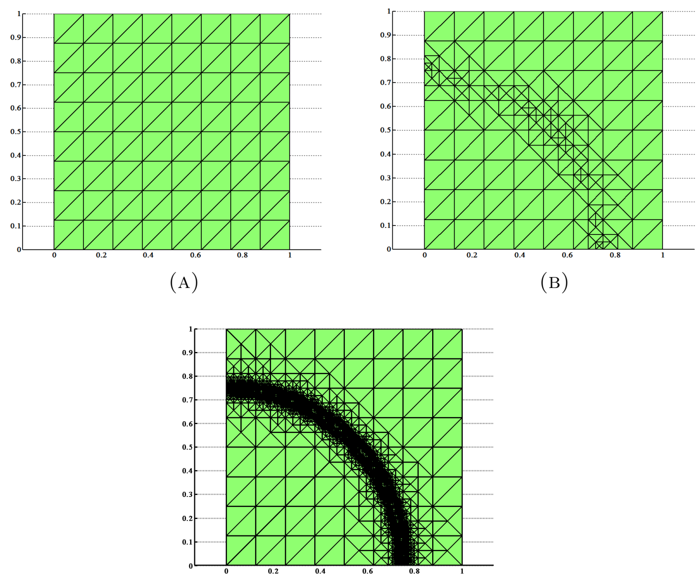

(A) (B) (C)

FIGURE 6. (A) initial mesh; (B) refined mesh after 10 refinements; (C) final mesh.

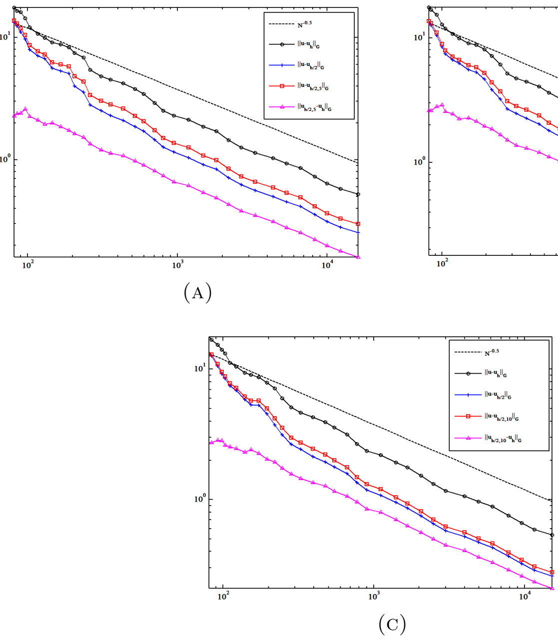

FIGURE 7. The convergence history of AFEM. (A) $m = 5$; (B) $m = 8$; (C) $m = 10$.

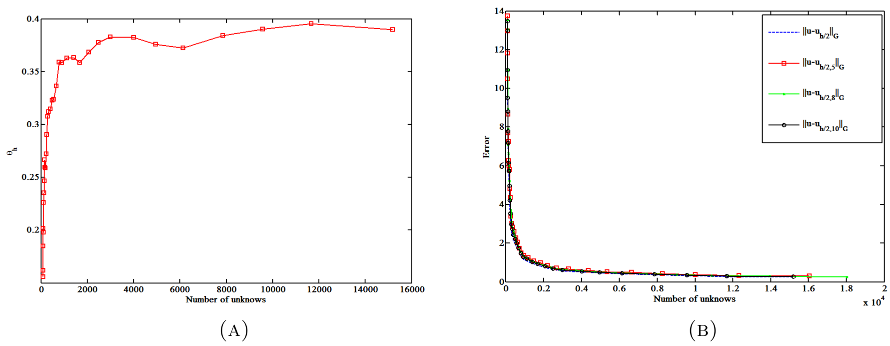

FIGURE 8. (A) The index θ_h for $m = 5$; (B) Errors $||u - u_{h/2,m}||_G$ for $m = 5, 8, 10$.

Example 3. We solve the model problem (3.1) in $\Omega = [-1, 1] \times [-1, 1]$, and take the exact solution to be

$$u = \frac{1}{x^2 + y^2 + 0.01}.$$

The results are shown in Figures 9, 10, and 11.

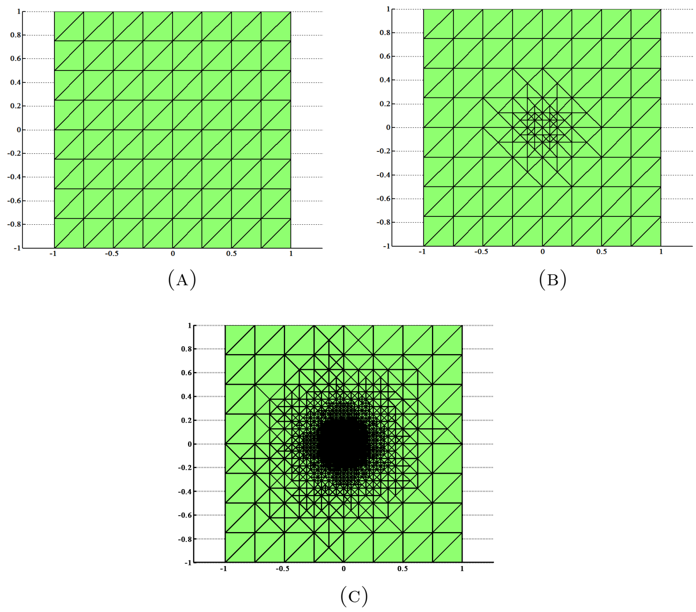

(A) (B) (C)

FIGURE 9. (A) initial mesh; (B) refined mesh after 10 refinements; (C) final mesh.

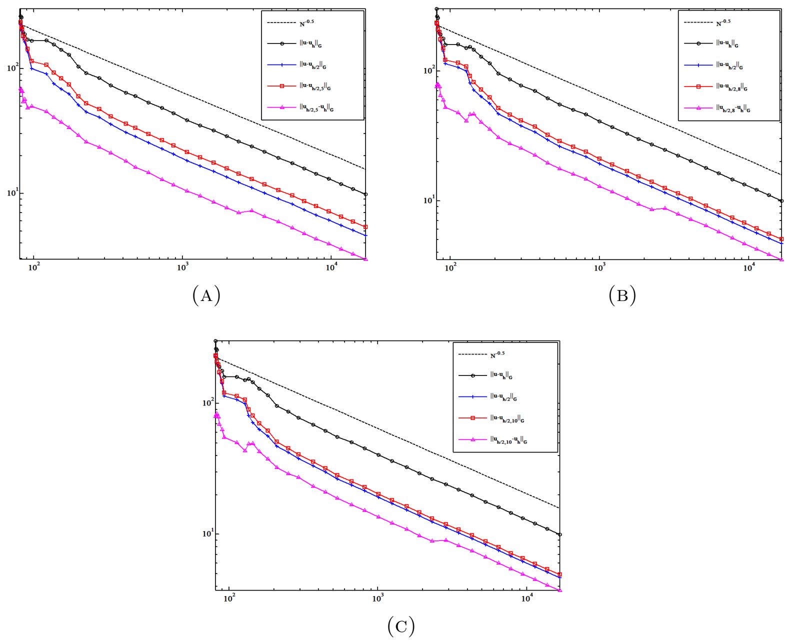

(A) (B) (C)

FIGURE 10. The convergence history of AFEM. (A) $m = 5$; (B) $m = 8$; (C) $m = 10$.

Acknowledgments.

The authors are very grateful to the anonymous referees for their insightful comments which improved our paper. This research work was partially supported

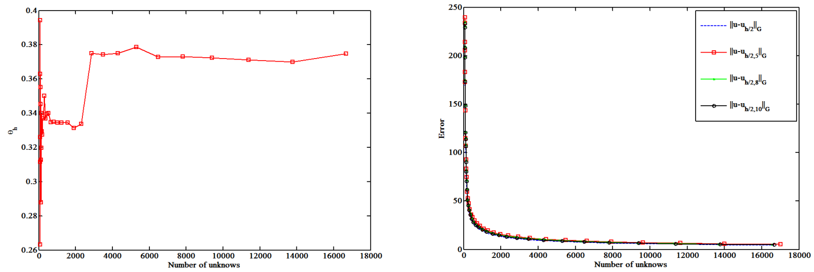

(A) (B)

FIGURE 11. (A) The index θ_h for $m = 5$; (B) Errors $||u - u_{h/2,m}||_G$ for $m = 5, 8, 10$.

by NSFC Key Project 91430213 and 91630205, NSFC Projects 11401506, 11771371 and 11771367, Hunan Education Department Project 15B236 and YB2015B027, Hunan NSF 2017JJ3304.

Reference.

[1] M. Ainsworth and J. T. Oden. *A Posteriori Error Estimation in Finite Element Analysis*. Wiley Interscience, New York, 2000.
[2] D. N. Arnold. An interior penalty finite element method with discontinuous elements. *SIAM J. Numer. Anal.*, 19:742–760, 1982.
[3] D. N. Arnold, F. Brezzi and B. Cockburn. Unified analysis of discontinuous Galerkin methods for elliptic problems. *SIAM J. Numer. Anal.*, 39:1749–1779, 2002.
[4] I. Babuška and W. C. Rheinboldt. *A posteriori* error estimates for the finite element method. *Int. J. Numer. Methods Eng.*, 12:1597–1615, 1978.
[5] I. Babuška and T. Strouboulis. *The Finite Element Method and Its Reliability*. Oxford University Press, Oxford, 2001.
[6] R. E. Bank. Hierarchical bases and the finite element method. *Acta Numer.*, 5:1–43, 1996.
[7] R. E. Bank and R. K. Smith. *A posteriori* estimates based on hierarchical basis. *SIAM J. Numer. Anal.*, 30:921–935, 1993.
[8] R. E. Bank and A. Weiser. Some *a posteriori* error estimators for elliptic partial differential equations. *Math. Comp.*, 44:283–301, 1985.
[9] L. Chen. *iFEM: An innovation finite element method package in Matlab*. http://math.uci.edu/ chenlong/iFem.html, 2008.
[10] C. M. Chen and Y. Q. Huang. *High Precision Finite Element Theory*. Hunan, 1994.
[11] Y. L. Chi, C. W. Shu. A phase-based interior penalty discontinuous Galerkin method for the Helmholtz equation with spatially varying wavenumber. *Comput. Methods Appl. Mech. Engrg.*, 318:456–473, 2017.
[12] L. C. Evans. *Partial Differential Equations: Second Edition*. World Book Inc., Beijing, 2010.
[13] M. J. Grote, A. Schneebeli and D. Schötzau. Interior penalty discontinuous Galerkin method for Maxwell's equations: Energy norm error estimates. *ScienceDirect. J. Comput. Math.*, 204:375–378, 2007.
[14] R. Hartmann and P. Houston. Symmetric interior penalty DG methods for the compressible Navier-Stokes equations I: method formulation. *Int. J. Numer. Anal. Model.*, 3(2006):1–20, 2005.
[15] R. Hartmann and P. Houston. An optimal order interior penalty discontinuous Galerkin discretization of the compressible Navier-Stokes equations. *J. Comput. Phys.*, 227:9670–9685, 2008.
[16] P. Houston, I. Perugia, A. Schneebeli and D. Schötzau. Interior penalty method for the indefinite time-harmonic Maxwell equations. *Numer. Math.*, 100(3):485–518, 2005.
[17] Y. Q. Huang and J. C. Li. Interior penalty discontinuous Galerkin method for Maxwell's equations in cold plasma. *J. Sci. Comput.*, 41:321–340, 2009.
[18] Y. Q. Huang, J. C. Li and W. Yang. Interior penalty DG methods for Maxwell's equations in dispersive media. *J. Comput. Phys.*, 230(12):4559–4570, 2011.

[19] Y. Q. Huang, H. Y. Wei, W. Yang and N. Y. Yi. A new *a posteriori* error estimate for adaptive finite element methods. *Domain Decomposition Methods in Science and Engineering XIX*, 63–74, 2010.
[20] O. A. Karakashian and F. Pascal. *A posteriori* error estimates for a discontinuous Galerkin approximation of second-order elliptic problems. *SIAM J. Numer. Anal.*, 41:2374–2399, 2003.
[21] A. Plaza, S. Falcn, J. P. Suárez and P. Abad. A local refinement algorithm for the longest-edge trisection of triangle meshes. *Math. Comput. Simul.*, 82(12):2971–2981, 2012.
[22] B. Rivière and M. F. Wheeler. *A posteriori* error estimates and mesh adaptation strategy for discontinuous Galerkin methods applied to diffusion problems. *Universtity of Texas at Austin Usa*, 2000.
[23] M. C. Rivara. Mesh refinement processes based on the generalized bisection of simplices. *SIAM J. Numer. Anal.*, 21:604–613, 1984.
[24] R. Verfürth. *A Review of a Posteriori Error Estimation and Adaptive Mesh-refinment Techniques.* Wiley/Teubner, Stuttgart, 1996.
[25] N. N. Yan. *Superconvergence Analysis and a Posteriori Error Estimation in Finite Element Methods.* Science Press, Beijing, 2008.
[26] O. C. Zienkiewicz and J. Z. Zhu. The supercovergent patch recovery and a posteriori estimates. *Int. J. Numer. Methods Eng.*, 33:1331–1382, 1992.

Hunan Key Laboratory for Computation and Simulation in Science and Engineering, Xiangtan University, Xiangtan 411105, P.R.China
E-mail: yangweixtu@126.com

Hunan Key Laboratory for Computation and Simulation in Science and Engineering, Xiangtan University, Xiangtan 411105, P.R.China
E-mail: lulingcao@163.com

Hunan Key Laboratory for Computation and Simulation in Science and Engineering, Xiangtan University, Xiangtan 411105, P.R.China
E-mail: huangyq@xtu.edu.cn

Department of Applied Mathematics, The Hong Kong Polytechnic University, Hung Hom, Hong Kong

The Hong Kong Polytechnic University Shenzhen Research Institute, Shenzhen 518057, P.R.China
E-mail: jintao.cui@polyu.edu.hk